

Thermal stability of carbon nanotubes

F. Xu · L. X. Sun · J. Zhang · Y. N. Qi ·
L. N. Yang · H. Y. Ru · C. Y. Wang ·
X. Meng · X. F. Lan · Q. Z. Jiao · F. L. Huang

Received: 15 September 2009 / Accepted: 1 April 2010 / Published online: 5 May 2010
© Akadémiai Kiadó, Budapest, Hungary 2010

Abstract Heat capacities of the carbon nanotubes (CNTs) with different sizes have been measured by modulated temperature differential scanning calorimetry (MDSC) and reported for the first time. The results indicated the values of C_p increased with shortening length of CNTs when the diameters of CNTs were between 60 and 100 nm. However, the values of C_p of CNTs were not affected by their diameter when the lengths of CNTs were 1–2 μm , or not affected by the length of CNTs when their diameters were below 10 nm. The thermal stabilities of the CNTs have been studied by TG-DTG-DSC. The results of TG-DTG showed that thermal stabilities of CNTs were enhanced with their diameters increase. With lengths increase, the thermal stabilities of CNTs increased when their diameters were between 60 and 100 nm, but there is a slight decrease when their diameters were less than 60 nm. The further DSC analyses showed both released heat and T_{onset} increased with the increase of CNTs diameters, which confirms the consistency of the

results from both TG-DTG and DSC on CNTs thermal stability.

Keywords CNTs · Heat capacity · Thermodynamic properties · Thermal stability · MDSC · TG-DTG-DSC

Introduction

Since the discovery of carbon nanotubes (CNTs) in 1991 by Iijima [1], CNTs have attracted a great deal of interest for their intrinsic properties and their possible applications. They are promising materials for various applications such as field emission, cold cathode, vacuum microelectronics applications, analytical biosensor, hydrogen storage, and so on [2–5]. Therefore, studies on their thermal stabilities were of quite importance. Literature [6] reported the thermal stability of single-wall carbon nanotubes (SWNTs) in air. The results showed that the SWNTs placed in air for 5 days were transformed into the amorphous carbon, and SWNTs were unstable in air and easily oxidized. Chang et al. [7] studied thermal decomposition of carbon nanotube/ Al_2O_3 powders using DSC. Comparing results on carbon powder (C), commercial carbon nanotubes (CBT), and an innovative composite of CNT on Al_2O_3 powders (CCNT), they thought CCNT was a safer material (less thermal hazard) than both C and CBT. At the same time, their results also implied that different types of carbon like C, CBT, and CCNT could yield different energies during thermal decomposition.

Up to now, no report about thermal stability, heat capacity, and thermodynamic properties of the CNTs with different sizes has been found in the literature. Thermal stability of materials is extraordinary significant for their practical applications. Molar heat capacities of the materials

F. Xu · H. Y. Ru · C. Y. Wang · X. Meng ·
X. F. Lan · Q. Z. Jiao
Chemistry and Chemical Engineering College, Liaoning Normal
University, 850 Huanghe Road, 116029 Dalian, People's
Republic of China

L. X. Sun (✉) · J. Zhang · Y. N. Qi · L. N. Yang
Materials and Thermochemistry Laboratory, Dalian Institute
of Chemical Physics, Chinese Academy of Sciences,
457 Zhongshan Road, 116023 Dalian, People's Republic of
China
e-mail: lxsun@dicp.ac.cn

F. L. Huang
State Key Laboratory of Explosion Science and Technology,
Beijing Institute of Technology, 100081 Beijing, People's
Republic of China

at different temperatures are very important basic data in both chemistry and engineering. Therefore, heat capacities determinations of various compounds have attracted many researchers' attention [8–12]. Furthermore, many other thermodynamic properties such as enthalpy and entropy can be calculated from the measured data of heat capacities.

In this article, thermal stabilities of CNTs with different diameters and lengths were studied by TG-DSC. Molar heat capacities of the CNTs were measured by MDSC and reported for the first time. The accuracy of MDSC is established by comparing the measured heat capacities of standard sapphire (Al_2O_3) with previously reported values (NIST) [13].

Experimental

Samples

All CNTs (see Table 1 for their description) were purchased from Shenzhen Nanotech Prot Co., Ltd. and were used without further purification.

Heat capacity measurement

Measurement of heat capacities of materials by MDSC has been reported [14, 15]. In this article, molar heat capacities of the CNTs were investigated by MDSC on DSC Q1000 (T-zero DSC-technology, TA Instruments Inc., USA). The DSC Q1000 operated in a temperature range from 220 to 473 K with a liquid nitrogen cooling system. And dry nitrogen gas was used as a purge gas (50 mL min^{-1}) through the DSC cell. The CNT samples mass was in the range 2–13 mg. Samples were weighed on a METTLER TOLEDO balance (AB135-S, Classic) with an accuracy of $\pm 0.01 \text{ mg}$. The samples were packed down and sealed in aluminum solid pans, and an empty aluminum pan was used as a reference. The pans were heated at a rate of 3 K min^{-1} according the following program: equilibrated at 173.15 K, modulated at $\pm 0.5 \text{ K}$ every 100 s, kept isothermal for 5 min, and then heated to 473.15 K.

The temperature of the equipment was initially calibrated in the standard DSC mode, using extrapolated onset

Table 1 The CNTs were used for measurement

Specimen	Diameter/nm	Length/ μm	Purity/%
S1 (MWNT)	60–100	5–15	≥ 95
S2 (MWNT)	60–100	1–2	≥ 95
S3 (MWNT)	40–60	5–15	≥ 95
S4 (MWNT)	40–60	1–2	≥ 95
S5 (MWNT)	<10	5–15	≥ 95
S6 (MWNT)	<10	1–2	≥ 95

temperatures of the melting of indium (429.75 K) at a heating rate of 10 K min^{-1} . The heat flow rate was calibrated with the heat of fusion of indium (28.45 J g^{-1}). The heat capacity calibration was made by running a standard sapphire (Al_2O_3) at each temperature. The coefficients for determining heat capacity from 173.15 to 473.15 K are: $K_{\text{total}} = 1.024$; $K_{\text{reversible}} = 1.019$.

Thermal analysis

A thermogravimetric analyzer (Model: Setsys 16/18, SETARAM Co., France) was used for TG-DSC measurement of these samples in the air with a flow rate of 30 mL min^{-1} . The heating rate was 10 K min^{-1} . The mass of the sample was about 1–2 mg. Two Al_2O_3 crucibles were used (capacity: $100 \mu\text{L}$). The reference crucible was filled with $\alpha\text{-Al}_2\text{O}_3$ (alfa-allumina). The TG equipment was calibrated by the $\text{CaC}_2\text{O}_4 \cdot \text{H}_2\text{O}$ (calcium oxalate monohydrate, 99.9%).

Results and discussion

Heat capacity of standard sapphire ($\alpha\text{-Al}_2\text{O}_3$)

Measurements of heat capacities of each sample were repeated for three times unless stated elsewhere. The emphasis of this study is to assess the reproducibility and to ensure accuracy of the measured data using MDSC (Q1000). The heat capacities of standard sapphire ($\alpha\text{-Al}_2\text{O}_3$) were reported at an interval of $\Delta T = 10 \text{ K}$ for the facile comparison with the literature values. The data of three reduplicate experiments and the experimental standard deviations for standard sapphire are given in Table 2. For sapphire measurement, the experimental relative standard deviations are below $\pm 0.5\%$. It shows that the testing system of MDSC is steady. The average capacity values of three runs ($C_p(\text{exp})$) and the recommended data ($C_p(\text{rec})$) of the National Institute of Standards and Technology (NIST) [13] are displayed in Fig. 1. Relative deviations (RD (%)) were calculated by the following equation:

$$\text{RD}(\%) = \frac{C_p(\text{exp}) - C_p(\text{rec})}{C_p(\text{rec})} \times 100 \quad (1)$$

The results showed that the relative deviations of our data from the recommended value (NIST) over the whole temperature range were within $\pm 1.5\%$.

Heat capacities of CNTs

The heat capacities of CNTs (S1, S2, S5, S6) were measured by DSC Q-1000 over the temperature range

Table 2 Comparison of the experimental heat capacities with the recommended value (NIST) for standard sapphire

T/ K	$C_p/\text{J g}^{-1} \text{K}^{-1}$				$C_p/\text{J g}^{-1} \text{K}^{-1}$ [13]	RD/%
	Dataset1	Dataset2	Dataset3	Average		
223	0.5745	0.5763	0.5804	0.5771	0.5684	1.5
233	0.5984	0.6002	0.6045	0.6010	0.5996	0.24
243	0.6254	0.6274	0.6316	0.6281	0.6294	-0.20
253	0.6532	0.6547	0.6572	0.6550	0.6577	-0.41
263	0.6797	0.6824	0.6839	0.6820	0.6846	-0.38
273	0.7078	0.7095	0.7103	0.7092	0.7102	-0.14
283	0.7343	0.7358	0.7358	0.7353	0.7344	0.12
293	0.7596	0.7615	0.7619	0.7610	0.7574	0.47
303	0.7819	0.7834	0.7850	0.7834	0.7792	0.54
313	0.8026	0.8047	0.8067	0.8047	0.7999	0.60
323	0.8228	0.8249	0.8254	0.8244	0.8194	0.60
333	0.8412	0.8416	0.8429	0.8419	0.8380	0.47
343	0.8571	0.8569	0.8598	0.8579	0.8556	0.27
353	0.8730	0.8732	0.8750	0.8737	0.8721	0.19
363	0.8859	0.8876	0.8897	0.8877	0.8878	-0.0075
373	0.9002	0.9002	0.9040	0.9015	0.9027	-0.14
383	0.9129	0.9129	0.9159	0.9139	0.9168	-0.32
393	0.9242	0.9244	0.9288	0.9258	0.9302	-0.47
403	0.9356	0.9363	0.9406	0.9375	0.9429	-0.57
413	0.9457	0.9454	0.9506	0.9472	0.9550	-0.81
423	0.9569	0.9560	0.9612	0.9580	0.9666	-0.89
433	0.9665	0.9647	0.9710	0.9674	0.9775	-1.0
443	0.9759	0.9746	0.9820	0.9775	0.9879	-1.1
453	0.9858	0.9846	0.9913	0.9872	0.9975	-1.0
463	0.9958	0.9922	1.001	0.9963	1.0074	-1.1

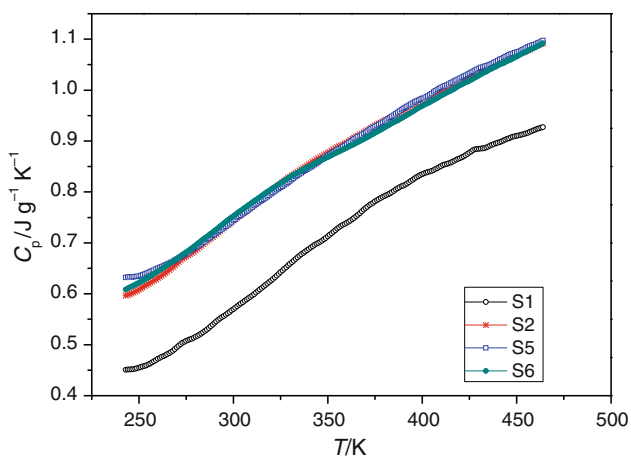


Fig. 1 Specific heat capacity, C_p , versus absolute temperature, T , for different samples of carbon nanotubes

220–470 K. The relative standard deviations for three parallel experiments were obtained which were below $\pm 2.3\%$ for S1, $\pm 1.9\%$ for S2, $\pm 1.5\%$ for S5, and

$\pm 0.93\%$ for S6. It shows reasonably good reproducibility in the temperature range from 220 to 470 K. The average heat capacities of above samples are plotted in Fig. 1. From Fig. 1, it can be seen that the heat capacities of these samples increase with increasing temperature, and no phase transition or thermal anomaly is observed, which indicates that these samples are stable in this temperature region. Figure 1 also indicates the values of C_p increase with reducing the length of CNT when the diameter of CNT is in 60–100 nm, and are not affected by the length of CNT when the diameter of CNT is below 10 nm. The values of C_p of CNTs (diameter is below 10 nm, length equals 5–15 or 1–2 μm) are almost the same as the ones of CNTs (diameter 60–100 nm and length 1–2 μm) in the given temperature range.

The heat capacities of these samples are fitted to the Shomate Equation of heat capacities (C_p) with reduced temperature (t) by means of the nonlinear least squares fitter using the OriginPro 7.5 software:

From 220 to 470 K for S1:

$$C_p (\text{J g}^{-1} \text{K}^{-1}) = -6.41956 + 33.6156t - 53.8473t^2 + 92.4000t^3 + 0.0861000/t^2 \quad (2)$$

where $t = T/1,000$, and T/K is the experimental temperature. The correlation coefficient of the fitting, $R^2 = 0.9999$, and a Chi-square (χ^2) per degree of freedom (DOF) for this fitting, i.e., $\chi^2/\text{DOF} = 3.13 \times 10^{-6}$. Relative deviations of the fitting heat capacity values from the experimental heat capacity values are within $\pm 9.5\%$ for S1 over the whole temperature range.

Based on Eq. 2, the heat capacity of S1 was calculated at 298.15 K to be $0.5641 \text{ J g}^{-1} \text{K}^{-1}$. The calculated thermodynamic properties (relative to 298.15 K) are listed in Table 3, where heat capacities (C_p) were calculated according to Eq. 2, $H - H_{298.15}$ and $S - S_{298.15}$ were derived from the following equations:

$$H - H_{298.15} = 1,000 \int_{0.29815}^t C_p dt \quad (3)$$

$$S - S_{298.15} = \int_{0.29815}^t \frac{C_p}{t} dt \quad (4)$$

From 220 to 470 K for S2:

$$C_p (\text{J g}^{-1} \text{K}^{-1}) = -6.90249 + 42.3329t - 83.1463t^2 + 59.1342t^3 + 0.0750200/t^2 \quad (5)$$

The correlation coefficient of the fitting, $R^2 = 0.9999$, and $\chi^2/\text{DOF} = 2.28 \times 10^{-6}$. Relative deviations are within $\pm 5.1\%$ for S2. Based on Eq. 5, the heat capacity of S2 was calculated at 298.15 K to be $0.7391 \text{ J g}^{-1} \text{K}^{-1}$. The calculated thermodynamic properties (relative to 298.15 K) for S2 are also listed in Table 3.

Table 3 Thermodynamic parameters of S1 and S2 in the temperature range 220–470 K

<i>T</i> /K	S1			S2		
	$C_p/J\ g^{-1}\ K^{-1}$	$H - H_{298.15}/J\ g^{-1}$	$S - S_{298.15}/J\ g^{-1}\ K^{-1}$	$C_p/J\ g^{-1}\ K^{-1}$	$H - H_{298.15}/J\ g^{-1}$	$S - S_{298.15}/J\ g^{-1}\ K^{-1}$
245	0.4509	-26.51	-0.09755	0.5977	-35.34	-0.1301
250	0.4559	-24.24	-0.08839	0.6084	-32.33	-0.1179
255	0.4626	-21.95	-0.07930	0.6201	-29.26	-0.1058
260	0.4708	-19.61	-0.07024	0.6325	-26.13	-0.09360
265	0.4803	-17.24	-0.06119	0.6455	-22.93	-0.08143
270	0.4909	-14.81	-0.05211	0.6591	-19.67	-0.06924
275	0.5025	-12.32	-0.04300	0.6729	-16.34	-0.05702
280	0.5148	-9.782	-0.03383	0.6871	-12.94	-0.04477
285	0.5278	-7.176	-0.02461	0.7014	-9.471	-0.03248
290	0.5412	-4.503	-0.01531	0.7157	-5.929	-0.02016
295	0.5551	-1.763	-0.005943	0.7301	-2.314	-0.007802
298.15	0.5641	0.0000	0.0000	0.7391	0.0000	0.0000
300	0.5693	1.048	0.003505	0.7444	1.372	0.004588
305	0.5838	3.931	0.01304	0.7586	5.130	0.01701
310	0.5984	6.886	0.02265	0.7727	8.958	0.02946
315	0.6130	9.915	0.03234	0.7865	12.86	0.04193
320	0.6277	13.02	0.04211	0.8002	16.82	0.05443
325	0.6423	16.19	0.05195	0.8136	20.86	0.06694
330	0.6568	19.44	0.06187	0.8267	24.96	0.07946
335	0.6712	22.76	0.07185	0.8396	29.12	0.09199
340	0.6854	26.15	0.08190	0.8522	33.35	0.1045
345	0.6993	29.61	0.09201	0.8644	37.65	0.1171
350	0.7130	33.14	0.1022	0.8764	42.00	0.1296
355	0.7264	36.74	0.1124	0.8881	46.41	0.1421
360	0.7395	40.41	0.1226	0.8994	50.88	0.1546
365	0.7523	44.14	0.1329	0.9105	55.40	0.1671
370	0.7647	47.93	0.1432	0.9213	59.98	0.1795
375	0.7767	51.78	0.1536	0.9318	64.62	0.1920
380	0.7883	55.70	0.1639	0.9420	69.30	0.2044
385	0.7996	59.67	0.1743	0.9520	74.04	0.2168
390	0.8104	63.69	0.1847	0.9618	78.82	0.2291
395	0.8208	67.77	0.1951	0.9714	83.65	0.2414
400	0.8309	71.90	0.2055	0.9807	88.53	0.2537
405	0.8404	76.08	0.2159	0.9899	93.46	0.2659
410	0.8496	80.30	0.2262	0.9990	98.43	0.2781
415	0.8583	84.57	0.2366	1.008	103.5	0.2903
420	0.8666	88.88	0.2469	1.017	108.5	0.3024
425	0.8745	93.24	0.2572	1.0255	113.6	0.3145
430	0.8820	97.63	0.2675	1.0342	118.8	0.3266
435	0.8890	102.1	0.2777	1.0429	124.0	0.3386
440	0.8956	106.5	0.2879	1.0517	129.2	0.3505
445	0.9018	111.0	0.2981	1.0604	134.5	0.3625
450	0.9077	115.5	0.3082	1.0693	139.8	0.3744
455	0.9131	120.1	0.3183	1.0782	145.2	0.3862
460	0.9181	124.7	0.3283	1.0873	150.6	0.3981

Table 4 Thermodynamic parameters of S5 and S6 in the temperature range 220–470 K

<i>T</i> /K	S5			S6		
	$C_p/J\text{ g}^{-1}\text{ K}^{-1}$	$H - H_{298.15}/J\text{ g}^{-1}$	$S - S_{298.15}/J\text{ g}^{-1}\text{ K}^{-1}$	$C_p/J\text{ g}^{-1}\text{ K}^{-1}$	$H - H_{298.15}/J\text{ g}^{-1}$	$S - S_{298.15}/J\text{ g}^{-1}\text{ K}^{-1}$
245	0.6297	-35.97	-0.1325	0.6081	-35.94	-0.1323
250	0.6354	-32.80	-0.1197	0.6200	-32.87	-0.1199
255	0.6425	-29.61	-0.1071	0.6325	-29.74	-0.1075
260	0.6507	-26.38	-0.09453	0.6452	-26.54	-0.09509
265	0.6600	-23.10	-0.08205	0.6583	-23.28	-0.08268
270	0.6701	-19.78	-0.06962	0.6715	-19.96	-0.07025
275	0.6809	-16.40	-0.05723	0.6848	-16.57	-0.05781
280	0.6923	-12.97	-0.04486	0.6982	-13.11	-0.04535
285	0.7043	-9.476	-0.03250	0.7115	-9.585	-0.03287
290	0.7166	-5.924	-0.02014	0.7248	-5.994	-0.02038
295	0.7292	-2.310	-0.007788	0.7379	-2.337	-0.007881
298.15	0.7373	0.0000	0.0000	0.7461	0.0000	0.0000
300	0.7421	1.368	0.004575	0.7509	1.385	0.004630
305	0.7551	5.111	0.01695	0.7637	5.171	0.01715
310	0.7682	8.919	0.02933	0.7764	9.022	0.02967
315	0.7813	12.79	0.04173	0.7888	12.93	0.04219
320	0.7945	16.73	0.05414	0.8010	16.91	0.05471
325	0.8076	20.74	0.06656	0.8130	20.94	0.06722
330	0.8206	24.81	0.07899	0.8247	25.04	0.07972
335	0.8335	28.94	0.09142	0.8362	29.19	0.09221
340	0.8463	33.14	0.1039	0.8475	33.40	0.1047
345	0.8589	37.41	0.1163	0.8585	37.67	0.1171
350	0.8714	41.73	0.1288	0.8693	41.98	0.1296
355	0.8836	46.12	0.1412	0.8799	46.36	0.1420
360	0.8956	50.57	0.1537	0.8903	50.78	0.1544
365	0.9074	55.08	0.1661	0.9005	55.26	0.1667
370	0.9190	59.64	0.1785	0.9105	59.79	0.1790
375	0.9303	64.27	0.1909	0.9204	64.37	0.1913
380	0.9415	68.95	0.2033	0.9302	68.99	0.2036
385	0.9523	73.68	0.2157	0.9398	73.67	0.2158
390	0.9630	78.47	0.2281	0.9493	78.39	0.2280
395	0.9734	83.31	0.2404	0.9588	83.16	0.2401
400	0.9836	88.20	0.2527	0.9682	87.98	0.2522
405	0.9936	93.14	0.2650	0.9776	92.84	0.2643
410	1.003	98.14	0.2772	0.9871	97.75	0.2764
415	1.013	103.2	0.2894	0.9965	102.7	0.2884
420	1.022	108.3	0.3016	1.006	107.7	0.3004
425	1.031	113.4	0.3138	1.016	112.8	0.3124
430	1.040	118.6	0.3259	1.025	117.9	0.3243
435	1.049	123.8	0.3380	1.035	123.0	0.3362
440	1.058	129.1	0.3500	1.045	128.2	0.3481
445	1.067	134.4	0.3620	1.056	133.5	0.3600
450	1.075	139.7	0.3740	1.066	138.8	0.3718
455	1.084	145.1	0.3859	1.077	144.1	0.3837
460	1.092	150.6	0.3978	1.088	149.6	0.3955

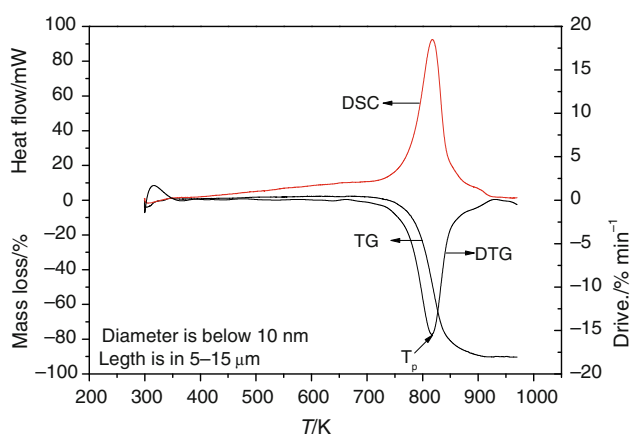


Fig. 2 The curves of TG-DTG-DSC for S5

From 220 to 470 K for S5:

$$C_p \text{ (J g}^{-1} \text{ K}^{-1}\text{)} = -5.88546 + 33.8297t - 60.2741t^2 + 39.1378t^3 + 0.0761900/t^2 \quad (6)$$

The correlation coefficient of the fitting, $R^2 = 0.9999$, and $\chi^2/\text{DOF} = 1.96 \times 10^{-6}$. Relative deviations are within $\pm 6.8\%$ for S5. Based on Eq. 6, the heat capacity of S5 was calculated at 298.15 K to be $0.7373 \text{ J g}^{-1} \text{ K}^{-1}$. The calculated thermodynamic properties (relative to 298.15 K) for S5 are listed in Table 4.

From 220 to 470 K for S6:

$$C_p \text{ (J g}^{-1} \text{ K}^{-1}\text{)} = -5.37595 + 35.3330t - 72.8248t^2 + 55.1556t^3 + 0.0532800/t^2 \quad (7)$$

The correlation coefficient of the fitting, $R^2 = 0.9996$, and $\chi^2/\text{DOF} = 8.54 \times 10^{-6}$. Relative deviations are within $\pm 8.3\%$ for S6. Based on Eq. 7, the heat capacity of S6 was calculated at 298.15 K to be $0.7642 \text{ J g}^{-1} \text{ K}^{-1}$. The calculated thermodynamic properties (relative to 298.15 K) for S6 are also listed in Table 4.

Thermal analysis of the CNTs (S1, S2, S3, S4, S5, and S6)

The curves of TG-DTG-DSC were obtained through the thermogravimetric analyzer (Model: Setsys 16/18, SETARAM Co., France) for S1, S2, S3, S4, S5, and S6 (see

Fig. 2), and their analytic results are listed in Table 5. For example, Fig. 2 is the curves of TG-DTG-DSC of S5, in which T_p is a peak temperature of DTG. Its process of mass loss through heating at oxygen atmosphere is completed by one step. S5 starts its mass loss after 790 K, and then attains tranquilization after 971 K. The total mass loss is 94.7%. The mass loss is because of the reaction between carbon and oxygen to release CO_2 .

From Table 5, it shows the temperature ranges of mass loss of S1 (790–971 K), S2 (775–959 K), S3 (753–954 K), S4 (767–956 K), S5 (717–917 K), and S6 (728–900 K) are higher than the ones of amorphous carbon (591–643 K) [6]. This result is attributed to the orbit of sp^2 completely combines between carbon and carbon in CNTs, so the temperature for carbon from CNTs reacts with oxygen is higher than that of amorphous carbon with oxygen at the same condition. From their quantity of mass loss, it also shows the purities of these CNTs are much higher than 94%. According to the curves of TG-DTG, it can be found that the ranges of decomposing temperature move toward higher temperature in air with increasing diameters of CNTs while T_p also increases at the same time. These results elucidate the thermal stabilities of CNTs are enhanced with the diameters of CNTs becoming larger. This is attributed to the surface area of CNT decreased while the diameter of CNT becomes larger, leading to the contacting area between CNT and air to be reduced, and finally resulting in thermal stability of CNT to be enhanced. With length becoming longer, the thermal stabilities of CNTs increase when the diameters are 60–100 nm; but the thermal stabilities decrease when the diameters are below 60 nm.

Furthermore, there is an exothermic peak on the DSC curve of CNTs. It indicates that there is an exothermic reaction for CNTs reacting with oxygen. Quantity of heat release and T_{onset} through CNTs reacting with oxygen slightly increases with the diameters of CNTs increasing; it also elucidates the thermal stabilities of CNTs are enhanced with increasing the diameters of CNTs. The result is in good agreement with the above one of TG-DTG analysis. But the exothermic quantity is independent of lengths of CNTs. The rule of changes of T_{onset} in DSC curve is the same as that of T_p .

Table 5 The results of thermal analysis

CNTs diameter/nm	TG-DTG					DSC				
	Ranges of decomp./K		T_p /K		$\Delta M/\%$		$T_{\text{onset}}/\text{K}$		$\Delta H/\text{kJ g}^{-1}$	
	Length 5–15 μm	Length 1–2 μm	Length 5–15 μm	Length 1–2 μm	Length 5–15 μm	Length 1–2 μm	Length 5–15 μm	Length 1–2 μm	Length 5–15 μm	Length 1–2 μm
60–100	790–971	775–959	931.6	926.9	98.4	97.9	867.0	855.4	24.29	24.04
40–60	753–954	767–956	906.0	920.6	97.3	98.3	836.3	843.5	22.43	22.34
<10	717–917	728–900	819.2	841.0	94.7	95.5	774.9	803.8	21.37	21.44

Conclusions

The heat capacities and TG-DTG-DSC curves were measured for CNTs with different sizes. The results indicated the values of C_p were increased with shortening the length of CNTs when the diameters of CNTs are between 60 and 100 nm. C_p of CNTs are not affected by the diameters when their lengths are 1–2 μm , C_p of CNTs are independent of their lengths when the diameters are below 10 nm. According to the results of TG-DTG, thermal stabilities of the CNTs are enhanced with their diameters increase. With length increase, the thermal stabilities of CNTs increase when the diameters are 60–100 nm. But the thermal stabilities appreciably decrease when the diameters are below 60 nm. The results of DSC analysis show the heat release increases with the diameter of CNT increase, but it is not affected by the lengths of CNTs. The results of thermal stability of CNTs by DSC are consistent with the ones obtained by TG-DTG.

Acknowledgements The authors gratefully acknowledge the financial supports to this study of National Natural Science Foundation of China (No. 20833009, U0734005, 20873148, 20903095, 50901070), 973 projects of China (No. 2010CB631303), Dalian Scientific Project (2009A11GX052), and the State Key Laboratory of Explosion Science and Technology, Beijing Institute of Technology (Grant No. KFJJ10-1Z).

References

- Iijima S. Helical microtubules of graphitic carbon. *Nature*. 1991; 354:56–8.
- Dillon AC, Jones KM, Bekkedahl TA, Kiang CH, Bethune DS, Habeen MJ. Storage of hydrogen in single-walled carbon nanotubes. *Nature*. 1997;386:377–9.
- Liu C, Fan YY, Liu M, Cong HT, Cheng HM, Dresselhaus MS. Hydrogen storage in single-walled carbon nanotubes at room temperature. *Science*. 1999;286:1127–9.
- Darkrim FL, Malbrunot P, Tartaglia GP. Review of hydrogen storage by adsorption in carbon nanotubes. *Int. J Hydrogen Energy*. 2002;27:193–202.
- Suw YL. Detection of dopamine in the pharmacy with a carbon nanotube paste electrode using voltammetry. *Bioelectrochemistry*. 2006;68:227–31.
- Liu H, Liu ZC, Liu JP. Investigations on stability of single-walled carbon nanotubes. *J Synth Cryst (Chin)*. 2006;35:494–6.
- Chang CW, Tseng JM, Horng JJ, Shu CM. Thermal decomposition of carbon nanotube/ Al_2O_3 powders by DSC testing. *Compos Sci Technol*. 2008;68:2954–9.
- Bessergenev VG, Kovalevskaya YA, Lavrenova LG, Paukov IE. Low temperature heat capacity of the coordination compound—nickel(II) nitrate with 4-amine-1,2,4-triazole at temperatures from 11 to 317 K. *J Therm Anal Calorim*. 2004;75:331–6.
- Tokoro N, Yamashita S, Igashira-Kamiyama A, Fujioka J, Konno T, Nakazawa Y. Low-temperature heat capacity of heptacopper(II) complex $[\text{Cu}-7(\mu(3)-\text{Cl})(2)(\mu(3)-\text{OH})(6)-(d\text{-pendisulfide})(3)]$. *J Therm Anal Calorim*. 2010;99:149–52.
- Leitner J, Ruzicka K, Sedmidubsky D, Svoboda P. Heat capacity, enthalpy and entropy of calcium niobates. *J Therm Anal Calorim*. 2009;95:397–402.
- Paukov IE, Kovalevskaya YA, Boldyreva EV, Drebushchak VA. Heat capacity of beta-alanine in a temperature range between 6 and 300 K. *J Therm Anal Calorim*. 2009;98:873–6.
- Arita Y, Ogawa T, Tsuchiya B, Matsui T. Heat capacity measurement and DSC study of hafnium hydrides. *J Therm Anal Calorim*. 2008;92:403–6.
- Archer DG. Thermodynamic properties of synthetic sapphire ($\alpha\text{-Al}_2\text{O}_3$), standard reference material 720 and the effect of temperature-scale differences on thermodynamic properties. *J Phys Chem Ref Data*. 1993;22:1441–53.
- Ike Y, Seshimo Y, Kojima S. Complex heat capacity of non-Debye process in glassy glucose and fructose. *Fluid Phase Equilibria*. 2007;256:123–6.
- Divi S, Chellappa R, Chandra D. Heat capacity measurement of organic thermal energy storage materials. *J Chem Thermodyn*. 2006;38:1312–26.